Fuzzy-based integrated zero-order shape optimization of steel–concrete–steel sandwich beams

Ishan Jha* and Krishna K. Pathak

Department of Civil Engineering, Indian Institute of Technology-Banaras Hindu University, Varanasi 221 005, India

This study presents a fuzzy-based integrated zero-order approach for shape optimization of steel–concrete–steel (SCS) sandwich beams. The method works on the novel idea of changing the shape of faceplates and core at the interface without affecting the overall shape of the beams. The proposed zero-order shape optimization technique is based on perpendicular growth and shrinkage in the design boundary at the interface of the faceplate and core to obtain an optimized shape. The concept of 'design elements' has been used to avoid mesh distortion. Automatic mesh generation and refinement are incorporated at each iteration. Fuzzy set theory is used to control the movement of nodes and convergence monitoring. A target maximum shear stress value (σ_t) is taken up and the shape is changed such that maximum shear stress (σ) at any point is smaller than or equal to the σ_t. For this, fuzzy membership functions in the form of triangular shape function have been used. The proposed approach coded in FORTRAN is labelled as gradientless shape optimization (GSO). It is found to perform effectively in determining the optimized shape of faceplates and core. To explain the efficacy of the proposed method, a few examples have been taken with changing boundary conditions and shape of the SCS sandwich beam.

Keywords: Design elements, fuzzy membership function, sandwich beams, shape optimization, zero-order approach.

A steel–concrete–steel (SCS) sandwich beam is made up of two steel faceplates of the thickness (t_f) sandwiching a concrete core of thickness (t_c), generally in the ratio of $t_f/t_c \ll 1$, connected via mechanical connectors forming a compact unit to withstand externally applied loads. The idea of a SCS sandwich beam was first introduced by Solomon *et al.*[1], using a SCS sandwich roadway slab in long and medium span composite bridges to decrease the overall weight of the structure. Since then, there has been a lot of research and development in SCS sandwich construction. One of the significant fields in the work on sandwich constructions has been optimization for a lighter weight sandwich structure. Weight of sandwich beams has been optimized using various methods, of which some used constraints like maximum allowable deflection, shear stress and bending stress[2], a few used criteria of simultaneous failure of the face and core of the sandwich beam[3], while others focused on reducing the face and core thickness[4,5] presenting 'small deflection theory' for the determination of deformation and stresses in sandwich beams[6]. Many researchers used lightweight core and optimized the density of the core to get an overall lesser weight[7–9]. Steeves[10] and Sjølund *et al.*[11] combined the geometry and core density optimization for sandwich beams which reduced the overall weight of beams more effectively. The use of honeycomb-shaped cores has been proposed by Al-Fatlawi *et al.*[12] for weight reduction of about 15% to 38%, and this was further optimized by Kondratiev and Gaidachuk[13] as irregularly shaped hexagonal honeycomb filler, which further reduced the weight by 2.1–12.3%. Other methods like optimizing stacking sequence in a multi-sandwich-panel composite structure[14] have also been used to enhance the strength of sandwich beams. In the work done on optimization of sandwich structures, two primary criteria have been focused upon, the first being the minimization of core density and the second being reduction in the thickness of the face and core. However, most of the research and its applications have stuck to the idea of having a constant face and core thickness. Nevertheless, with the advent of modern and improved fabrication techniques, the demand for using lighter weight design has intensified, and sandwich elements with non-uniform cross-section will likely be used. The weight density of steel (around 7750 kg/m^3) is very high compared to concrete (around 2500 kg/m^3). Hence, reducing the amount of steel and replacing it with concrete can serve the purpose of a lighter weight SCS sandwich beam. However, this should be done such that the structural integrity and serviceness of the structure are not hampered.

The non-gradient/zero-order method has long been in use for the optimization of structures. There are various studies where shape optimization has been performed using different zero-order methods[15]. Non-gradient methods have been employed by some researchers using an idea inspired by the 'living structures', where they proposed adding material to areas of higher stress while subtracting material from areas of lower stress to get an optimum

*For correspondence. (e-mail: ishan.jha.rs.civ18@iitbhu.ac.in)

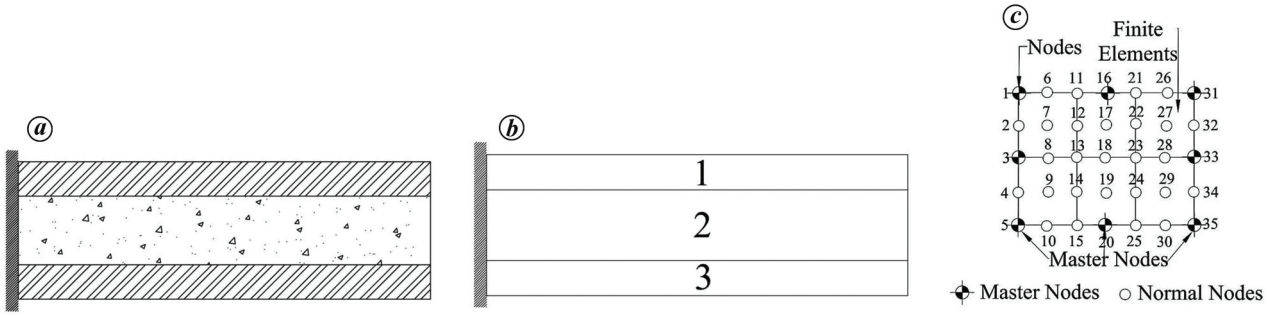

Figure 1. ***a***, Steel–concrete–steel (SCS) sandwich cantilever beam. ***b***, Division of the model into design elements 1, 2 and 3. ***c***, Sub-division of design element no. 1 into finite elements.

shape of the structure[16–19]. Zhixue[20] proposed a zero-order method for shape optimization, taking into consideration the minimization of stress concentration factor. Frequency constraint to obtain the optimized shape of truss structures was used by Lingyun *et al*.[21]. Nagy *et al.*[22] proposed an isometric analysis for shape optimization of the beam, altering both weight of the structure and spatial location of the control point to obtain the optimized shape. Methods like harmony search[23], genetic algorithms[24] and bacterial foraging algorithms[25] have been reported as effective non-gradient methods for shape optimization. Inspired by the studies on non-gradient methods for shape optimization, the present study proposes a novel idea of changing the shape of faceplates and core on the interface. For this integrated zero-order method is used aiming towards reducing the amount of steel and increasing the amount of concrete used without affecting the overall shape of the beam to have a lighter weight SCS sandwich beam.

Integrated zero-order method

The integrated zero-order method focuses on the efficiency of optimization and its flexibility to different sets of initial intricacies. It targets the geometric representation of the boundary of the model in a convenient manner. The feature of automatic mesh generation and re-meshing of the model at every iteration has been incorporated in this approach. We have also used an optimum number of design nodes and design elements so as to have a faster convergence without any compromise in the accuracy of results[26]. This approach is compiled in a FORTRAN code, and the software is labelled as gradientless shape optimization (GSO).

Model generation

While generating a finite element model for shape optimization, it is necessary to monitor the shape of the model after each iteration for which new mesh is generated, discarding the older mesh, as the older mesh will not be valid for the next iteration for stress analysis. The changed boundary shape results in possible distortion of elements and newer geometric and loading conditions, which can only be dealt with using an updated finite element mesh. For these above-mentioned criteria, the isoparametric mapping technique[27,28] is used with the design element concept so as to assure that the design variable which controls the finite element mesh also controls the optimization model[27,28].

In this methodology, the SCS structure subjected to optimization is first partitioned into the required number of design elements. Then each design element is characterized by a set of keynodes or master nodes, which is responsible for controlling the geometry of the design elements. The design elements are further divided into smaller finite elements using the master nodes. Figure 1 shows the different stages of discretization of the beam.

A two-dimensional isoparametric interpolation function is used to characterize the boundary of these design elements. Every design element bears eight master nodes. The master nodes present at the boundaries, which are to be taken into consideration for optimization, are treated as design nodes. The design nodes have their respective coordinates; these coordinates are considered as design variables. The isoparametric mapping is used to obtain the coordinates for the generated nodal points. Let X and Y be the coordinates for the generated nodal points. Then

$$\left.\begin{aligned} X &= \sum_{i=1}^{N_m} N_i(\xi,\eta)\cdot X_i \\ Y &= \sum_{i=1}^{N_m} N_i(\xi,\eta)\cdot Y_i \end{aligned}\right\}, \tag{1}$$

where X_i and Y_i represent the coordinates of the master node i, ξ and η represent the natural coordinates in accordance to the point (X, Y), N_i represents the shape function and N_m represents the number of master nodes present in that design element. From eq. (1), it can be inferred that the master nodes control the generated finite element mesh, and hence the geometry changes according to the

changed coordinates of the master nodes. The optimizer gives the modified coordinates of the master nodes which at each iteration are sent to the mesh generator for generation of a new mesh to be used by the finite element program. In the present study we have used nine-noded Lagrangian elements for finite element modelling to get a good compromise between simplicity of use and accuracy of the result.

Fuzzy membership function

In the zero-order method for shape optimization, the modification of geometry is greatly dependent upon the stress at the boundary nodes. The geometry is modified at each iteration taking into consideration the value of maximum shear stress at the design nodes in the previous iteration. The criterion of maximum shear stress (σ) being less than or equal to the target maximum shear stress (σ_t) is fulfilled when the value of σ at each design node is almost equal to the σ_t value. Achieving this state of stress is uncommon and difficult, as it is roughly in fuzzy form. To overcome this, the fuzzy set theory has been employed to carry out the nodal movement of the geometry. In order to find the shape for which the σ value is nearest to the σ_t value, the concept of fuzzy membership function is used[29]. In this study, the triangular shape membership function has been used.

Triangular shape membership function

In a triangular shape membership function, a linear relationship is obtained between the membership value (μ) and σ_t. The value of μ becomes equal to 1, if σ for the design nodes is equal to σ_t (Figure 2). This can be expressed mathematically by eq. (2)

$$\mu(\sigma) = \begin{cases} \dfrac{\sigma}{\sigma_t} & \text{if } \sigma < \sigma_t \\ 1 & \text{if } \sigma = \sigma_t \\ 2 - \dfrac{\sigma}{\sigma_t} & \text{if } \sigma_t < \sigma < 2\sigma_t \\ 0 & \text{if } \sigma > 2\sigma_t \end{cases}. \tag{2}$$

When σ is greater than σ_t, the material is added and when σ is lesser than σ_t, the material is subtracted in each iteration until the values of both σ at the design nodes and σ_t become more or less equal. This approach is incorporated using a fuzzy membership concept taking in *i*th node movement to be proportionate to the move factor (MF). In the present study, the difference allowed between the values of σ and σ_t is less than or equal to 0.01 N/mm^2. MF is expressed by eq. (3)

$$\left.\begin{aligned} &\text{If } \sigma_t > \sigma_t,\ \text{MF} = \{\mu(\sigma_t) - 1\} \\ &\text{If } \sigma_t < \sigma_t,\ \text{MF} = \{1 - \mu(\sigma_t)\} \end{aligned}\right\}. \tag{3}$$

Figure 3 shows the MF versus stress plot.

Figure 4 shows the direction of movement of the design nodes. Here node *j*, which is the middle node of Lagrangian elements, is selected as the direction node. The node *i*, which represents the design node, moves in accordance with the node *j*. The shortest distance between the design nodes and their respective direction nodes is represented by L_{min}, which can be expressed mathematically by eq. (4)

$$L_{\min} = \min_{i=1}^{N_d}(L_i), \tag{4}$$

where N_d is the number of design nodes and $L_i = \sqrt{(X_i - X_j)^2 + (Y_i - Y_j)^2}$.

The nodal movement in the study has been allowed as one-tenth of the full-length movement of L_{min}. Therefore, movement of the design nodes is represented by eq. (5)

$$\text{MV}(i) = 0.1 \cdot L_{\min} \cdot \text{MF}. \tag{5}$$

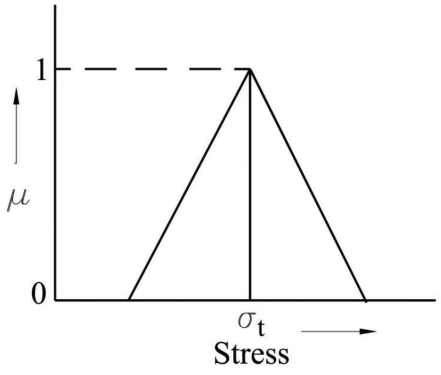

Figure 2. Triangular function.

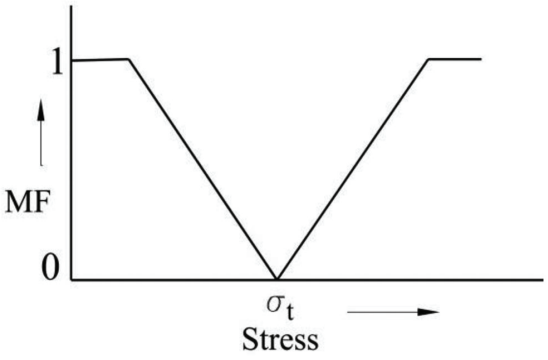

Figure 3. Move factor (MF).

Table 1. Comparison study of gradientless shape optimization with experimental results obtained by Solomon *et al.*[1] for interfacial shear stress and central deflection of different beam

Beams	B3	B5	B11	B12	B15	B17
Length (mm)	2000	2000	2000	2000	2000	2000
Width (mm)	150	150	150	300	150	150
Core depth (mm)	75	90	90	90	100	105
Plate thickness (mm)	3.18	3.18	3.18	3.18	4.76	4.76
E_{concrete} (kN/mm^2)	34.1	34.7	34.3	34.2	34.4	31.6
E_{steel} (kN/mm^2)	210	230	207	228	227	222
Shear span (mm)	225	90	750	150	750	750
Collapse load (kN)	45	195	42.3	145	46.6	45
Interfacial shear stress (N/mm^2) by Solomon *et al.*[1]	1.21	4.19	0.89	1.56	1	0.92
Present interfacial shear stress (N/mm^2)	1.57	4.37	0.94	1.59	1.17	1.04
Central deflection (mm) by Solomon *et al.*[1]	–	5.49	7.72	–	–	–
Present central deflection (mm)	1.89	5.57	7.44	1.19	5.14	4.41

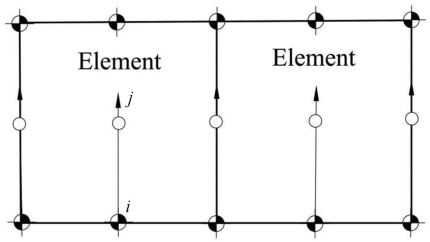

Figure 4. Direction node.

At each iteration, there is a change in the coordinates of the design node *i*. This can be represented by eq. (6)

$$\left.\begin{aligned} X_i' &= X_i + (X_j - X_i)\cdot\frac{\mathrm{MV}(i)}{L_i} \\ Y_i' &= Y_i + (Y_j - Y_i)\cdot\frac{\mathrm{MV}(i)}{L_i} \end{aligned}\right\}, \tag{6}$$

where X_i' and Y_i' are the newly obtained coordinates, and (X_i, Y_i) and (X_j, Y_j) are the coordinates for the direction node.

As the new coordinate value is obtained, data from the optimizer are sent to the mesh generator, where a new mesh is generated for further stress analysis. This process is repeated continuously until the criterion for convergence is reached.

Convergence criteria

The membership function value under ideal conditions should always be equal to 1, but because of the fuzzy nature it is difficult to achieve this condition. Hence for the purpose of convergence, fuzzy interaction, also termed as minimum membership function (MMF) has been utilized. The MMF value changes after each iteration and becomes maximum for the optimum shape. Hence when the MMF value starts decreasing at each iteration and continues to decrease up to three continuous iterations, then execution of the program stops and convergence criterion is considered to be achieved. This can be mathematically expressed by eq. (7)

$$\mu(\sigma_{\text{iter}}) = \min_{i=1}^{N_d}(\cap\mu(\sigma_i)), \tag{7}$$

If $\mu(\sigma_{\text{iter}}) < \mu(\sigma_{\text{iter}} + 1)$, continue optimization. If $\mu(\sigma_{\text{iter}}) > \mu(\sigma_{\text{iter}} + 1)$, stop optimization as the convergence is achieved.

Steps involved in the computation

The software follows the following steps:

1. Prepare the SCS model for which optimization is to be done with the assumption of proper connection between the faceplates and core.
2. Divide the model into the optimum required number of design elements.
3. Define the design nodes according to the criteria for shape optimization.
4. The minimum finite element mesh is generated according to the selected design nodes in order to obtain accurate but faster convergence.
5. Finite element analysis for the given boundary and loading conditions is carried out and MF values at the design nodes are calculated.
6. The boundary shape is optimized using the integrated zero-order method.
7. The changed coordinates of the new boundary shape are taken into consideration for the next iteration, and steps 4–6 are repeated.
8. The iteration stops when the convergence is reached to obtain the final optimized shape of the model.

Validation study

For performing the optimization process in SCS sandwich beams, it is necessary that the software is able to analyse

Table 2. Parameters for different sandwich beams with iterations and time required to obtain the optimized shape along with overall central deflection

Support condition	Type of loading	Type of sandwich beam	Live load (N)	Position of loading	Dimension (mm): L = Length, B = Breadth, D = Overall depth (face sheet, core, face sheet)	No. of iterations to obtain the optimized shape	System time taken to obtain the optimized shape (sec)	Central deflection before optimization (mm)	Central deflection after optimization (mm)
Fixed cantilever	Point load	Straight	1000	At the free end	$L = 750$, $B = 200$, $D = 180$ (15, 150, 15)	537	69.41	0.867×10^{-2}	0.947×10^{-2}
	Uniformly distributed load	Straight	1000	Along the length	$L = 750$, $B = 200$, $D = 180$ (15, 150, 15)	946	109.32	0.563×10^{-2}	0.587×10^{-2}
Simply supported	Point load	Straight	7000	At midpoint	$L = 1000$, $B = 300$, $D = 240$ (20, 200, 20)	117	15.99	0.107×10^{-1}	0.110×10^{-1}
		Curved	4000	At midpoint	$L = \cap 1000$, $B = 200$, $D = 240$ (20, 200, 20)	162	23.15	0.102×10^{-1}	0.108×10^{-1}
	Uniformly distributed load	Straight	7000	Along the length	$L = 1000$, $B = 300$, $D = 240$ (20, 200, 20)	262	31.82	0.719×10^{-2}	0.801×10^{-2}
		Curved	4000	Along the length	$L = \cap 1000$, $B = 200$, $D = 240$ (20, 200, 20)	312	43.65	0.722×10^{-2}	0.879×10^{-2}
Fixed	Point load	Straight	7000	At midpoint	$L = 1000$, $B = 300$, $D = 240$ (20, 200, 20)	331	44.25	0.483×10^{-2}	0.559×10^{-2}
		Curved	4000	At midpoint	$L = \cap 1000$, $B = 200$, $D = 240$ (20, 200, 20)	436	57.60	0.376×10^{-2}	0.468×10^{-2}
	Uniformly distributed load	Straight	7000	Along the length	$L = 1000$, $B = 300$, $D = 240$ (20, 200, 20)	476	63.07	0.262×10^{-2}	0.340×10^{-2}
		Curved	4000	Along the length	$L = \cap 1000$, $B = 200$, $D = 240$ (20, 200, 20)	736	98.61	0.204×10^{-2}	0.263×10^{-2}

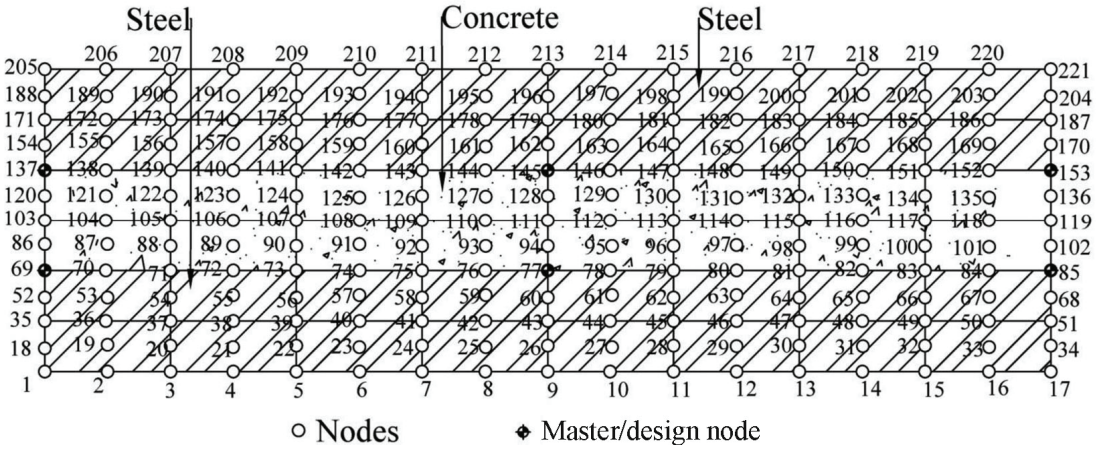

Figure 5. Schematic representation of SCS sandwich beam discretized in 48 nine-noded Lagrangian elements.

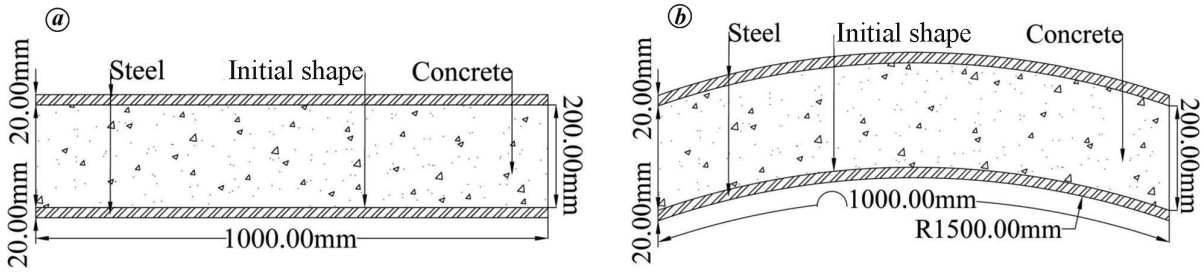

Figure 6. Initial shape of (***a***) straight and (***b***) curved SCS sandwich beams.

an SCS sandwich beam correctly. To prove the correctness of the software, a validation study is done where those results obtained by GSO software for interfacial shear stress and deflection are compared with those obtained by Solomon *et al.*[1] in their experimental work on SCS sandwich beams. Solomon *et al.*[1] designed different types of SCS sandwich beams, changing the thickness of the core and faceplates and analysed them experimentally for collapse load and deflection. They calculated the interfacial shear stress between steel face and concrete core. However, they reported the results of deflection for beams 5 and 11 only. Table 1 shows the comparative results obtained by Solomon *et al.*[1] and the present GSO results for SCS sandwich beams.

From Table 1, it can be successfully inferred that the results obtained by the present GSO software are in good agreement with those obtained by Solomon *et al.*[1]. Hence it can be utilized for the analysis of stress and deflection of SCS sandwich beams.

Numerical illustration

Using the proposed approach compiled in the GSO software, a few examples of shape optimization of SCS sandwich beams are provided. The Young's modulus for steel plates is taken as 2×10^5 N/mm^2 and the concrete core is taken as 2×10^4 N/mm^2. The weight density of steel is taken as 7900 kg/m^3 and concrete as 2400 kg/m^3. Table 2 presents the dimensions, applied live load and beam types. Three design elements have been considered in all the beams with appropriate design nodes. The fixed cantilever beam has been discretized into 36 nine-noded Lagrangian plane stress element forming a total of 169 nodes, whereas the fixed and simply supported beams are discretized into 48 nine-noded Lagrangian plane stress element forming a total of 221 nodes. Figure 5 is a schematic representation of beam discretized in 48 nine-noded Lagrangian elements. The value of σ_t in all the cases is taken as 0.3 N/mm^2 (according to the criteria of design shear strength of concrete without reinforcement in accordance to design code IS 456:2000 (ref. 30)). Figure 6 depicts the initial shape of the straight and curved SCS sandwich beams. Table 2 also shows the system time taken and the number of iterations in each case to obtain the optimized shape, along with the central deflection before and after optimization. Figures 7 and 8 show the optimized shape obtained and σ distribution in each case respectively.

Results and discussion

From the results in this study, it can be inferred that the GSO software can successfully optimize the given SCS

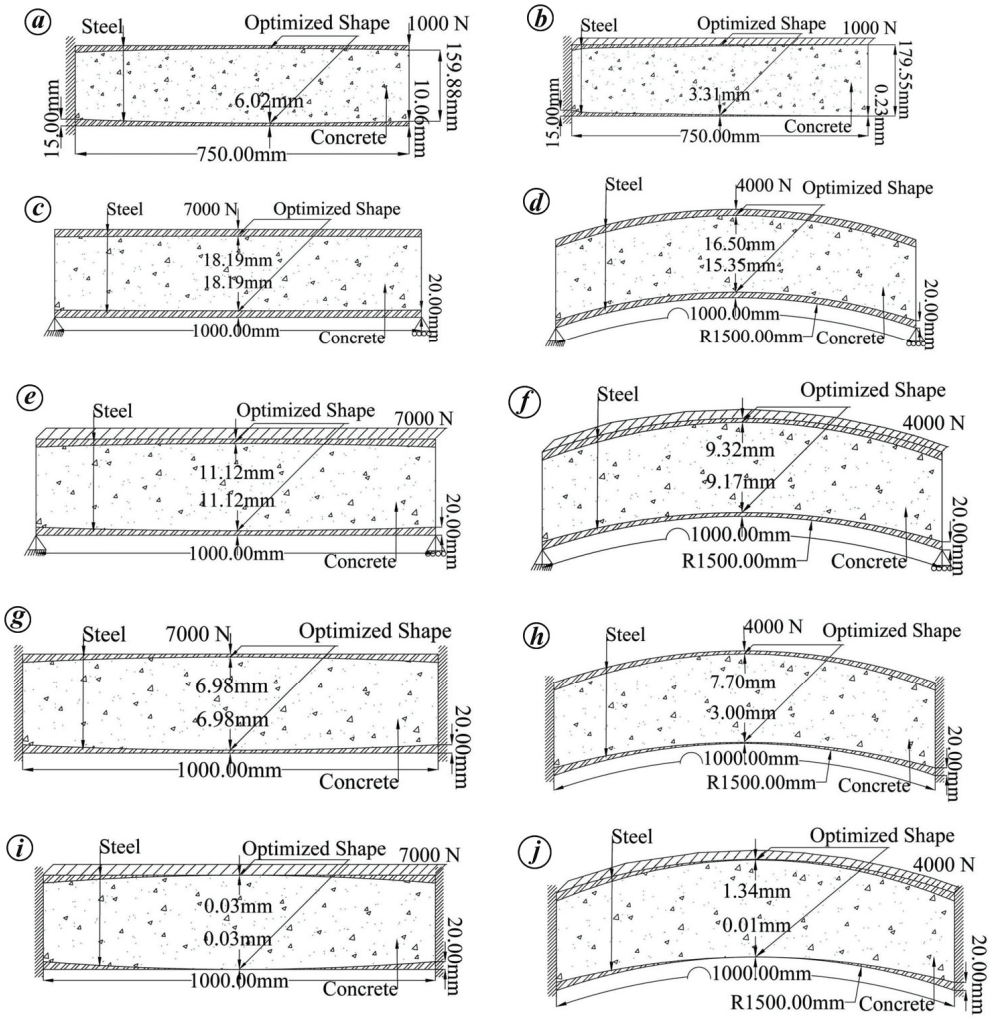

Figure 7. ***a***, ***b***, Fixed cantilever SCS sandwich beams with (***a***) point load and (***b***) uniformly distributed load. ***c***, ***d***, Simply supported (***c***) straight and (***d***) SCS sandwich beams with point load. ***e***, ***f***, Simply supported (***e***) straight and (***f***) curved SCS sandwich beams with uniformly distributed load. ***g***, ***h***, Fixed (***g***) straight and (***h***) curved SCS sandwich beams with point load. ***i***, ***j***, Fixed (***i***) straight and (***j***) curved SCS sandwich beams with uniformly distributed load.

sandwich beam satisfying the criterion of maximum shear stress being less than or equal to the target maximum shear stress at any point. From Figure 7 *a* and *b*, it can be observed that for the case of concentrated load on a cantilever SCS beam, the amount of steel removed from the faceplate is less than that in the case of similarly loaded but uniformly distributed load on the same cantilever SCS beam. Similar results are observed in the case of simply supported straight and curved SCS beams and fixed straight and curved SCS beams. It can also be seen that in the case of straight SCS beams, the upper and lower faceplates have been optimized to similar thickness, but in the case of curved SCS beam, the upper and lower faces are optimized to different thicknesses. For instance, in Figure 7 *h* it can be seen that the upper faceplate is optimized to a central thickness of 7.70 mm, whereas the lower faceplate is optimized to a central thickness of 3.00 mm. This is due to the nonlinear stress distribution in curved SCS beams. Also, it can be observed that the SCS sandwich beams with fixed support conditions are more optimized than those with simply supported support conditions for the same load. This is evident from the fact that for similar beams, a fixed supported beam can take more load than a simply supported beam. The change in deflection before and after optimization is also less, of the order 10^{-4}. Hence, the condition of serviceability is being satisfied. From the point of view of the GSO software, it can also be observed that the number of iterations required to reach the final optimized shape is more in the case of a uniformly distributed load than in the case of a concentrated load. However, the number of iterations in each case to reach the final optimized shape can be reduced by increasing the nodal movement from one-tenth of the full-length movement of $L_{\min}$ to one-fourth or even more; but

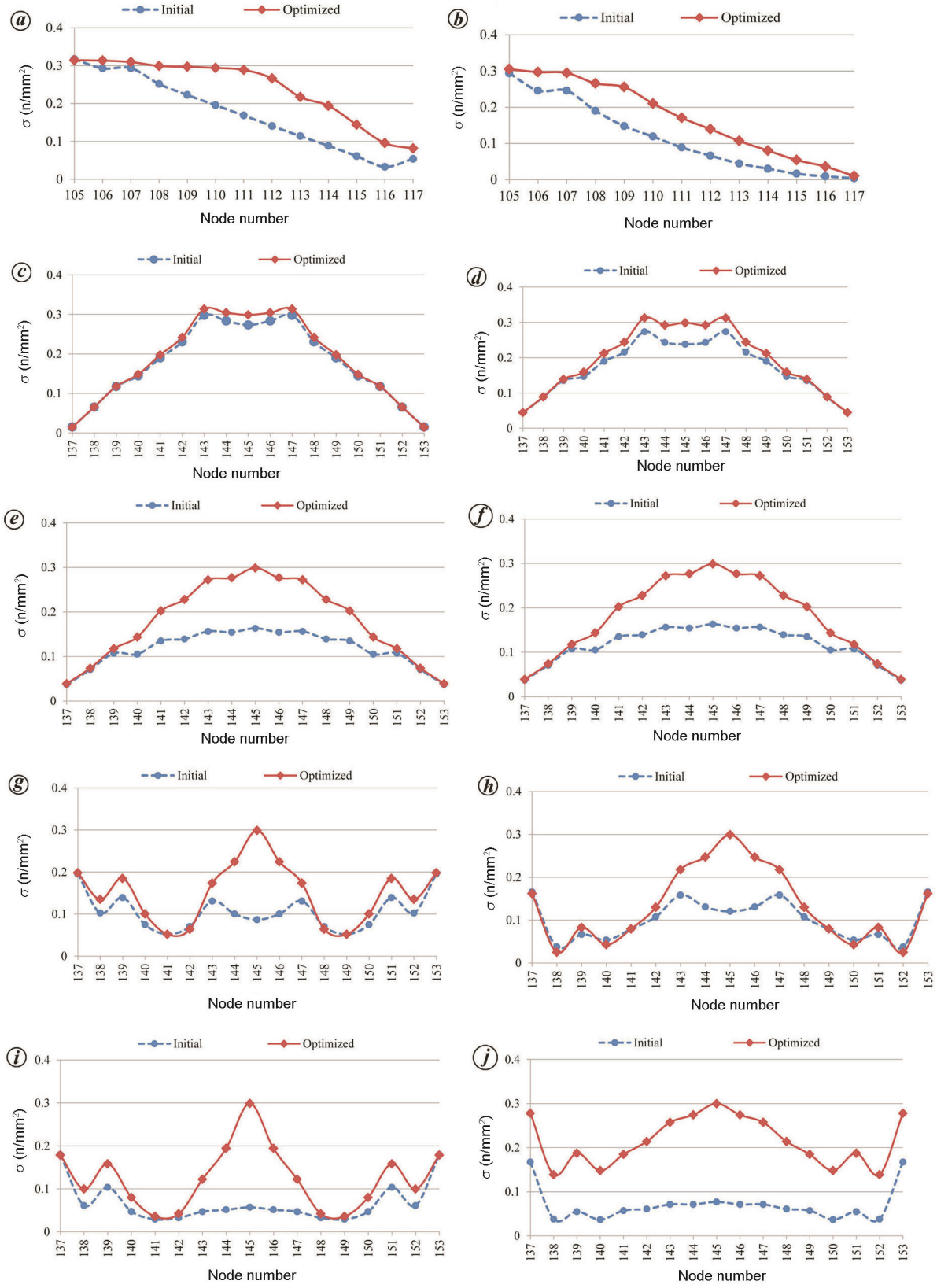

Figure 8. ***a***, ***b***, σ distribution in fixed cantilever SCS sandwich beams having (***a***) a point load and (***b***) uniformly distributed load. ***c***, ***d***, σ distribution in simply supported (***c***) straight and (***d***) curved SCS sandwich beams having a point load. ***e***, ***f***, σ distribution in simply supported (***e***) straight and (***f***) curved SCS sandwich beams having uniformly distributed load. ***g***, ***h***, σ distribution in fixed (***g***) straight and (***h***) curved SCS sandwich beams having a point load. ***i***, ***j***, σ distribution in fixed (***i***) straight and (***j***) curved SCS sandwich beams having uniformly distributed load.

this will impact the accuracy of the results in a minor way. Each iteration done by the GSO software on an average takes a runtime of approximately 1.406×10^{-1} sec.

Conclusion

This study discussed the fuzzy-based integrated zero-order method for shape optimization of SCS structures. This whole approach has been compiled as a software named GSO using FORTRAN code. The shape at the interface between the core and the faceplate is successfully optimized, lowering the amount of steel and increasing the amount of concrete for a certain load on the beam, keeping the overall cross-section of the beam the same. This helps in the reduction of the overall weight of the structure while fulfiling the criterion of structural integrity and serviceness. The value of σ_{max} obtained is near the σ_t taken, and nowhere does σ exceed the value of σ_t taken. The use of optimum design elements and proper design nodes has resulted in faster convergence without compromising on the quality of the results. The overall runtime of the program is also less and does not demand any high-end computing capabilities. The capabilities of the GSO software based on the integrated zero-order approach have been effectively demonstrated by a few examples. The proposed approach is found to carry out successful shape optimization of SCS sandwich beams under the novel approach of changing the shape at the interface of the face and core to have a SCS sandwich beam with reduced weight without changing the overall shape. It can also be used for industrial applications.

Conflict of interest. The authors declare no potential conflict of interest with respect to the research, authorship and publication of this article.

1. Solomon, S. K., Smith, D. and Cusens, A., Flexural tests of steel–concrete–steel sandwiches. *Mag. Concr. Res.*, 1976, **28**(94), 13–20.
2. Huang, S. N. and Alspaugh, D. W., Minimum weight sandwich beam design. *Am. Inst. Aeronaut. Astron. J.*, 1974, **12**(12), 1617–1618.
3. Triantafillou, T. C. and Gibson, L. J., Minimum weight design of foam core sandwich panels for a given strength. *Mater. Sci. Eng.*, 1987, **95**, 55–62.
4. Demsetz, L. A. and Gibson, L. J., Minimum weight design for stiffness in sandwich plates with rigid foam cores. *Mater. Sci. Eng.*, 1987, **85**, 33–42.
5. Hanifehzadeh, M. and Mousavi, M. M. R., Predicting the structural performance of sandwich concrete panels subjected to blast load considering dynamic increase factor. *J. Civil Eng., Sci. Technol.*, 2019, **10**(1), 45–58.
6. Paydar, N. and Park, G. J., Optimal design of sandwich beams. *Comput. Struct.*, 1990, **34**(4), 523–526.
7. Gibson, L. J., Optimization of stiffness in sandwich beams with rigid foam cores. *Mater. Sci. Eng.*, 1984, **67**(2), 125–135.
8. Swanson, S. R. and Jongman, K., Optimization of sandwich beams for concentrated loads. *J. Sandw. Struct. Mater.*, 2002, **4**(3), 273–293.
9. Bergan, P. G., Bakken, K. and Thienel, C., Analysis and design of sandwich structures made of steel and lightweight concrete. In III European Conference on Computational Mechanics (eds Motasoares, C. A. *et al.*), Springer, Dordrecht, The Netherlands, 2008, pp. 1–18.
10. Steeves, C. A., Optimizing sandwich beams for strength and stiffness. *J. Sandw. Struct. Mater.*, 2012, **14**(5), 573–595.
11. Sjølund, J. H., Peeters, D. and Lund, E., Discrete material and thickness optimization of sandwich structures. *Comp. Struct.*, 2019, **217**, 75–88.
12. Al-Fatlawi, A., Károly, J. and György, K., Structural optimization of a sandwich panel, design for minimum weight shipping and airplane containers. In MultiScience-XXXIII. microCAD International Multidisciplinary Scientific Conference, Miskolc, Hungary, 2019, pp. 1–10.
13. Kondratiev, A. and Gaidachuk, V., Weight-based optimization of sandwich shelled composite structures with a honeycomb filler. *East. Eur. J. Enterpr. Technol.*, 2019, **1/1**(97), 24–33.
14. Fan, H., Wang, H. and Chen, X., Optimization of multi-sandwich-panel composite structures for minimum weight with strength and buckling considerations. *Sci. Eng. Compos. Mater.*, 2018, **25**(2), 229–241.
15. Munk, D. J., Vio, G. A. and Steven, G. P., Topology and shape optimization methods using evolutionary algorithms: a review. *Struct. Multidiscip. Optim.*, 2015, **52**(3), 613–631.
16. Mattheck, C., Biological shape optimisation of mechanical components based on growth. In Proceedings of the International Congress on Finite Element Method, Baden-Baden, Germany, 1989, pp. 167–176.
17. Mattheck, C. and Erb, D., Shape optimisation of a rubber bearing. *Int. J. Fatigue*, 1991, **13**(3), 206–208.
18. Mattheck, C. and Burkhardt, S., A new method of structural shape optimisation based on biological growth. *Int. J. Fatigue*, 1990, **12**(3), 185–190.
19. Mattheck, C. and Burkhardt, S., Successful three-dimensional shape optimization of a bending bar with rectangular hole. *Fatigue Fract. Eng. Mater. Struct.*, 1992, **15**(4), 347–351.
20. Zhixue, W., An efficient approach for shape optimization of components. *Int. J. Mech. Sci.*, 2005, **47**(10), 1595–1610.
21. Lingyun, W., Mei, Z., Guangming, W. and Guang, M., Truss optimisation on shape and sizing with frequency constraints based on genetic algorithms. *Comput. Mech.*, 2005, **35**(5), 361–368.
22. Nagy, A. P., Abdalla, M. M. and Gürdal, Z., Isogeometric sizing and shape optimization of beam structures. In Structures, Structural Dynamics, and Materials Conference, Palm Springs, California, USA, 2009.
23. Lee, K. and Geem, Z., A new structural optimization method based on the harmony search algorithm. *Comput. Struct.*, 2004, **82**(9–10), 781–798.
24. Manan, A., Vio, G. A., Harmin, M. Y. and Cooper, J. E., Optimisation of aeroelastic composite structures using evolutionary algorithms. *Eng. Optim.*, 2010, **42**(2), 171–184.
25. Georgiou, G., Vio, G. A. and Cooper, J. E., Aeroelastic tailoring and scaling using bacterial forging optimisation. *Struct. Multidisc. Optim.*, 2014, **50**, 81–99.
26. Imam, M. H., Three-dimensional shape optimization. *Int. J. Numer. Methods Eng.*, 1982, **18**(5), 661–673.
27. Zienkiewicz, O. C. and Taylor, R. L., *The Finite Element Method, Vols 1&2*, McGraw Hill, London, UK, 1991, 4th edn.
28. Krishnamoorthy, C. S., *Finite Element Analysis Theory and Programming*, McGraw Hill, New Delhi, 1994.
29. Zimmermann, H. J., *Fuzzy Set Theory*, Kluwer, Dordrecht, The Netherlands, 1996.
30. IS 456:2000, Plain and reinforced concrete – code of practice.

Received 23 November 2020; revised accepted 5 August 2021

doi: 10.18520/cs/v121/i7/941-949